Deposited via The University of Leeds.

White Rose Research Online URL for this paper:
https://eprints.whiterose.ac.uk/id/eprint/116763/

Version: Accepted Version

Full Paper

# Process Analytical Tools to control polymorphism and particle size in batch crystallization processes

Thomas B. Hansen, Elena Simone, Zoltan K Nagy, and Haiyan Qu

1
2
3
4
5
6
7
8
9
10
11
12
13
14
15
16
17
18
19
20
21
22
23
24
25
26
27
28
29
30
31
32
33
34
35
36
37
38
39
40
41
42
43
44
45
46
47
48
49
50
51
52
53
54
55
56
57
58
59
60

# Process Analytical Tools to control polymorphism and particle size in batch crystallization processes

*Thomas B. Hansen\**[1]*, Elena Simone*[2]*, Zoltan Nagy*[3]*, Haiyan Qu*[1]

[THBH@kbm.sdu.dk](THBH@kbm.sdu.dk)

[1]*Department of Chemical Engineering, Biotechnology and Environmental Technology, University of Southern Denmark, Campusvej 55, 5230 Odense, Denmark;*
[2] *School of Food Science and Nutrition, University of Leeds, Leeds LS2 9JT, UK*
[3] *School of Chemical Engineering, Purdue University, West Lafayette, 47907, Indiana, United State*

**For Table of Contents Only**
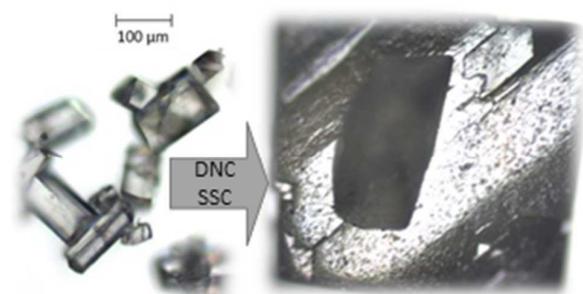
**Abstract**

In this work, Process Analytical Technology (PAT) based approaches for controlling the polymorphism and crystal size of a nonsteroidal anti-inflammatory drug (Piroxicam) during batch cooling crystallization has been investigated. Previously obtained results regarding the crystallization behaviour of the different polymorphs of Piroxicam in a small scale (100 ml) crystallizer have been used to design and to initiate the control approach described in this paper. The results of the present work demonstrated the challenge of reproducing the crystallization process with respect to the product polymorphism at different scales. The solute concentration has been proved to be a critical parameter in determining the polymorphism of Piroxicam in the small scale crystallization experiments; however, the same operation parameters could not yield the same polymorph in the crystallization in 2L crystallizers. Both Direct Nucleation Control (DNC) and Supersaturation Control (SSC) have been proved to be effective at controlling the polymorphism of Piroxicam in seeded cooling crystallization, furthermore, applying DNC also improved the particulate properties (larger crystal size).

**Keywords**: Crystallization, Polymorphism, Direct nucleation control (DNC), PAT, Piroxicam, Supersaturation control (SSC)

## 1. Introduction

As the complexity of new drugs is on the increase, issues with poor physicochemical properties are becoming a common obstacle in development[1]. One possibility of improving the performance of a drug candidate is to explore the various crystal forms of the compound, either on its own or in various complexes such as solvates or co-crystals[2–4]. Such exploration can be beneficial to drug development but these initial experiments are often carried out at a small scale. Additionally, although they do show what crystal forms the compound may exhibit and allow for investigations into the properties of these polymorphs, the control methods cannot simply be up-scaled for production.

Conducting reliable control of polymorphism throughout the developing and production process of an Active Pharmaceutical Ingredient (API) is a very challenging task. The issues with up-scaling are an ever-increasing challenge and failing to control the polymorphic form of an API can lead to foregoing development of a new product or, in the worst case, having a product on the market fail to reach quality control standard. In fact, different polymorphs can have different dissolution rates, solubility and they can present very different stability during storage[5]. Since the formation of a specific polymorphic form in solution crystallization is sensitive to the process conditions, the results obtained from small scale experiments often cannot be reproduced in a larger scale process. Although valuable knowledge regarding the polymorphic nature as well as the crystallization mechanisms of the different polymorphs can be obtained from small scale experiments, more sophisticated control strategies are required to ensure the polymorphic control in larger scale productions. It has been reported that Supersaturation Control (SSC) allows for cooling profiles that leads to a relatively low supersaturation during batch crystallization. This helps to avoid secondary nucleation and therefore both reduces the risk of unwanted polymorphs appearing, and yields fewer fine particles in the product[6–9].In cases where SSC is not sufficient to ensure the desired particle sizes or in cases where even a controlled cooling leads to unwanted polymorphs forming, controlled dissolution may be an option. This can either be done based on a fixed cooling profile where the temperature gradient is reversed to allow for the dissolution of smaller particles, or various process analytical technology (PAT) tools can be used to select when to start and stop the heating of the reactor. One technique is the use of particle counts from a Focused Beam Reflectance Measurement (FBRM) probe as this helps detecting when new crystals are being formed in the solution. When used in combination with seeding, this approach can be highly

effective as the seed crystals will generally ensure that the produced form is identical to the seed. At the same time, any new polymorphs that may nucleate out of solution would start out as small particles and quickly dissolve during the heating steps. This method of control is known as Direct Nucleation Control (DNC) and it has previously been used to control the crystallisation of organic compounds and to increase particle size and narrow the size distribution of the final product[10–15].It was also found to reduce the amount of solvent inclusion[11]. That all contributes to a more efficient production with less variation in product quality. In the present work, this method is only applied to a single step batch reactor, however the concept have been expanded to multistage mixed suspension in a continuous cooling crystallization[16,17] as well as used for anti-solvent and non-seeded crystallization[18].

The aim of this work is to demonstrate the effectiveness of PAT tools and PAT-based feedback control strategies in scaling up crystallisation processes for polymorphic compounds. Piroxicam was used as model compound. In our previous work, the crystallization of Piroxicam, which is a nonsteroidal anti-inflammatory drug (NSAID), has been investigated in a small scale (100 ml) crystallization system[19,20] Among the four polymorphs that Piroxicam can form[21–23], only the polymorphic form I and II, which possess difference intermolecular hydrogen bonding and molecular orientations, have been obtained in our previous work along with the monohydrate form which was obtained in cooling crystallization from solutions with high water concentration. It has been observed that the formation of Piroxicam polymorphic form I, form II and the monohydrate depends on various operating parameters, such as the solvent composition, solute concentration, presence of certain additives, and the way supersaturation is created (cooling crystallization or anti-solvent crystallization). A crystal form landscape for Piroxicam was established to demonstrate the link between the solvent composition, solute concentration, and the phase of the nucleated crystals. In the present work, the results obtained in the 100 mL scale system were compared to experiments conducted in a 2L crystallizer. Because of the impossibility to directly scale up the system seeding was conducted in the 2 L crystallizer to control the polymorphic purity of the end product. Finally, Direct Nucleation Control (DNC) and Supersaturation Control (SSC) strategies were tested. Both techniques were proved effective in controlling the polymorphic purity of Piroxicam during the experiments at large scale.

## 2.  Experimental methods

### 2.1  Materials and Equipment

Piroxicam was purchased from Hangzhou Hyper Chemicals Limited, Zhejiang, China, and identified as the polymorphic form II. Piroxicam form I was prepared using anti-solvent crystallization as described in previous literature[10].Raman spectroscopy was used in the present work to identify the solid form of the crystals produced in the experiments. As the link between solid forms and Raman spectra have previously been confirmed[24] by comparison with XRPD[212223] this method was found to be acceptable in determining crystal structure. All solvents were obtained from Sigma-Aldrich as 99.9% analytical grade solvents. For the anti-solvent experiments, deionised water was used.

All crystallization experiments were carried out in a 2L double walled glass reactor equipped with an overhead stirrer with a flat bottomed anchor type impeller and a thermostat and compared to experiments performed at 100 mL with magnetic stirring[10]. Anti-solvent addition was achieved using a peristaltic pump connecting the anti-solvent container to a stainless steel tube at the top of the reactor, slightly off-centre to the stirrer to ensure that anti-solvent would be added to the mixing vortex.

The process analytical technology (PAT) tools used for process monitoring and control include an FBRM G400 0.5−2000 μm (Mettler Toledo with iCFBRM software version 4.3), a ParticleView V19 PVM (Mettler Toledo with iCPVM version 7.0), Mettler Toledo, a Zeiss MCS621 UV/vis spectrophotometer with ATR-UV/vis (Attenuated total reflectance –Ultraviolet/Visible) 190−720 nm Zeiss probe (Zeiss ProcessXplorer software version 1.3-Build 1.3.1.30) and a RXN1 Raman immersion probe with 785 nm laser (Kaiser with iC Raman 4.1 software). The data from the FBRM and the Huber is

transmitted in real-time to the CryPRINS software (Crystallisation Process Informatics System) which allows real time temperature control and simultaneous monitoring of signals from different probes (FBRM, ATR-UV/Vis, thermocouple, conductivity probes and pH-meter). The pre- and post-processing of the data was done with Matlab R2012b and iC Raman 4.1. Filtered and dried crystals where analysed using a DXR Raman microscope (780nm, Thermo Scientific equipped with OMNIC 8 software). XRPD were obtained with a MiniFlex600XRPD from Rigaku with data collected from 5° to 50° at 0.02° step size. Final product particle size distribution was determined using a Beckman Coulter LS 13320 laser diffraction particle size analyser.

### 2.2  Anti-solvent crystallization
Anti-solvent crystallization experiments were performed by dissolving Piroxicam in pure acetone at a ratio that would yield a saturated solution at 25°C. Water was then added to the reactor as the anti-solvent. Before the anti-solvent crystallization started, the Piroxicam-acetone solution was heated to 35°C with stirring for 1 hour to dissolve all Piroxicam crystals. The temperature was then lowered to 27°C and once stabilized; the addition of anti-solvent was started. The feed rate of water to the reactor was fixed at 5 mL/min and samples were taken once nucleation was detected, and every 30 minutes thereafter. Samples were filtered, dried and analysed with the Raman microscope. Based on the initial results it was found that the first form to nucleate in significant quantities were form I, but transformation into the monohydrate would happen as more water was added. To increase the yield of form I, experiments were also carried out where the addition of water was stopped once nucleation was observed and the temperature of the reactor was lowered to 10°C to force more API out of solution.

### 2.3  Seeded and non-seeded cooling crystallization
Initially non-seeded cooling crystallization was carried out with low API concentration as this was previously found to produce form I crystals[19] in a small scale 100 mL reactor with a solid state thermostat, allowing for fast and precise temperature control. However, this result was not possible to be reproduced in the 2L crystallizer, probably due to the less effective cooling system. It was then decided to use polymorphic seeding to control the polymorphism of the product at this scale. The Piroxicam form I produced with the anti-solvent crystallization was used as the seeds. Form I seed crystals were added at 2°C above the calculated saturation temperatures of each batch and with a seed load of 10%. This allowed for faster production of large amounts of form I for later use in DNC and SSC experiments.

### 2.4  Direct Nucleation, and Supersaturation Control (DNC/SSC)
The direct nucleation control procedure has been widely used and explained in detail in the literature [11,25-29]. The technique uses both FBRM and CryPRINS to keep the number of total counts/s in the vessel constant during the batch crystallization process. The total counts/s measured by the FBRM is sent to CryPRINS and the temperature in the vessel is decreased if the measured total counts/s is lower than the set point range, or increased if it is higher (fine crystal particles are then dissolved). The total counts/s set point as well as the desired cooling and heating rate are set up in CryPRINS before starting the batch. Those parameters are usually system dependent and can be selected after a few preliminary trials.

For all experiments with active control, seed crystals were added to initiate the crystallization and DNC or SSC were then used to control the crystallization process. These two control strategy use two different features of the CryPRINS software and different in-line process analytical technology (PAT) probes, FBRM for the DNC and ATR-UV/Vis for the SSC strategy. In the DNC experiments presented in this work, seed crystals were added to saturated solutions and the FBRM total counts/s was left to stabilize with no temperature change. As the counts/s was found to be very low at the desired seed

load, two setups were tried. The high counts DNC used a set point of 1000±100 counts/s and the low counts set point was determined by the initial count from seed crystals (approx. 200±100 counts).

A calibration-free approach was used to perform the seeded supersaturation control (SSC) experiments[8,30]. An inferential solubility curve for Piroxicam was obtained by slowly heating up a slurry of Piroxicam form I in acetone from 5.5°C to 50°C (0.01°C/min). The amount of Piroxicam and acetone in the crystallizer corresponded to the solubility of Piroxicam at 40 °C, so all the solid Piroxicam dissolved at the end of the temperature profile. ATR-UV/Vis spectra were recorded and a polynomial relation was found between the first derivative of the spectra signal ($F$) at 306 nm (correlated with the Piroxicam concentration) and temperature ($T$). This correlation, $F = f(T)$, corresponds to an inferential solubility curve expressed as UV signal versus temperature, instead of the classical concentration versus temperature relationship, generally used in calibration-based supersaturation control, leading to the use of arbitrary units (a.u.).

The polynomial function measured is shown in Equation 1:

$$F_{formI} = 3.409 \cdot 10^{-7}T^2 + 1.383 \cdot 10^{-5}T + 6.685 \cdot 10^{-4} \qquad (1)$$

Equation (1) was implemented in the CryPRINS software and the experiments conducted followed the procedure:

1. Solid Piroxicam was added to pure acetone (about 0.045 g/g acetone, corresponding to a saturation temperature of around 43-45 °C) and the temperature was raised to 55 °C to allow complete dissolution of the solid;
2. The temperature was kept constant at 50 °C for about half an hour and then the system was cooled down to about 41 °C;
3. Crystalline seeds were added in an amount of about 10% of the total solid mass and the supersaturation control option in CryPRINS was switched on;
4. The supersaturation set point was adjusted during the first minutes of control in order to guarantee a reasonable batch time.

The supersaturation set point is calculated as the difference between the desired UV signal at a given temperature and the value of the inferential solubility of Piroxicam at that temperature. This value can be directly inserted in CryPRINS. Three different experiments were conducted in order to identify the optimal set point and seeding conditions.

## 3.  Results

In previous work[10] it was found that several methods can be used to control the polymorphism of Piroxicam in batch crystallization from acetone or mixtures of acetone and water. It has been observed that in cooling crystallization there is a strong link between the Piroxicam concentration and the polymorphism of the produced crystals. Higher solute concentration favoured the formation of form II, while form I was crystallized out from solutions with low concentration. The monohydrate Piroxicam was produced in cooling crystallization from acetone/water mixtures when water concentration exceeded 10%. It was also discovered that anti-solvent crystallization in the Piroxicam-acetone-water system could produce form I regardless of the high water concentration in the system and the presence of form II seed crystals. Polymorphic seeding has been proved very effective in directing the nucleation of form I and II in cooling crystallization and therefore can be used to control the polymorphism of Piroxicam in crystallization process.

These previous studies were, however, conducted in small scale reactors and with limited options for monitoring the system during nucleation. This also meant that no form of feedback control could be implemented. Nevertheless, feedback control strategy might be necessary for robust production of one specific polymorph, especially in cases where different forms were known to compete. In the present work, preliminary experiments were firstly conducted to test if the concentration-directed polymorphic cooling crystallization experiments performed at 100 mL scale can be re-produced in a larger scale (2 L) crystallization system. The difficulties of up-scaling crystallization processes are evident from the results as previous crystallization methodologies were found ineffective in the large scale system, where effective mixing and precise temperature control is more difficult to achieve. For this reason approaches for effective control of polymorphism were explored based on the in-depth understanding of the polymorphic crystallization mechanism obtained from the small scale experiments.

### 3.1 Cooling crystallization

Preliminary cooling crystallizations were performed at low Piroxicam concentration, which was previously found to favour the crystallization of form I at 100 mL scale. Although several experiments were conducted, and the operating conditions were close to what had previously been used at small scale, the produced crystals were consistently form II. A comparison of polymorphic behaviour along with operating conditions are shown in Table 1.This deviation from previous results could be attributed to the varied cooling efficiency and mixing condition in the 2 L crystallizer, as well as the different batch of Piroxicam from a different supplier. It was noted that the temperature difference between set point and actual reactor temperature was wider for the large scale set up as would be expected. Furthermore, temperature gradient could not be followed below 10°C where the cooling rate would start to abate. This could be one reason for the unexpected form II as the system would stay in the metastable zone for longer and at higher temperatures before nucleation occurred. Another likely factor was the change in raw material as the impurities contained in the material might affect the crystallization process. It was not possible to lower the concentration further to promote the crystallization of form I, as this would require sub-zero temperatures to even cross into a supersaturated range. It was therefore decided to use seeding to have robust control of the product polymorphism.

**Table 1 Polymorphic behaviour of Piroxicam in non-seeded cooling crystallization**

| Initial concentration [mg/g] | Cooling rate [K/min] | Polymorphic form nucleated at | |
|---|---|---|---|
| | | 100 mL scale | 2 L scale |
| 40 | 0.5 | Form II | Form II |
| 25 | 0.5 | Form I | Form II |
| 20 | 1.2 | Form I | Form II |

### 3.2 Anti-solvent crystallisation

As previously reported, anti-solvent crystallization of Piroxicam from acetone solution was found to yield form I even if form II seeds were added to the reactor[19]. In some cases, the monohydrate form was also found during anti-solvent experiments, although in very low quantities and only at 45°C. To further investigate the circumstances where monohydrate formation would become an issue, preliminary experiments were carried out using PVM to monitor the formation of the crystals. Surprisingly, these experiments showed that all three forms were present at some point during the crystallization process. It has previously been reported that polymorph II form needle shaped crystals, whereas form I crystallizes in a cubic structure[20,31]. As the initial crystals observed from PVM were needle shaped, this would indicate that form II nucleated first shortly after the first particles become visible via PVM, several needle shaped crystals can be seen (Figure 1). As the water addition continues, cubic crystals

start to dominate the solution and no increase in the amount of needles was seen. As the water concentration increase, the monohydrate form starts to appear at the end of the batch (Figure 1) seeming to either grow on the surface of the cubic form I crystals or at least agglomerating to these particles.
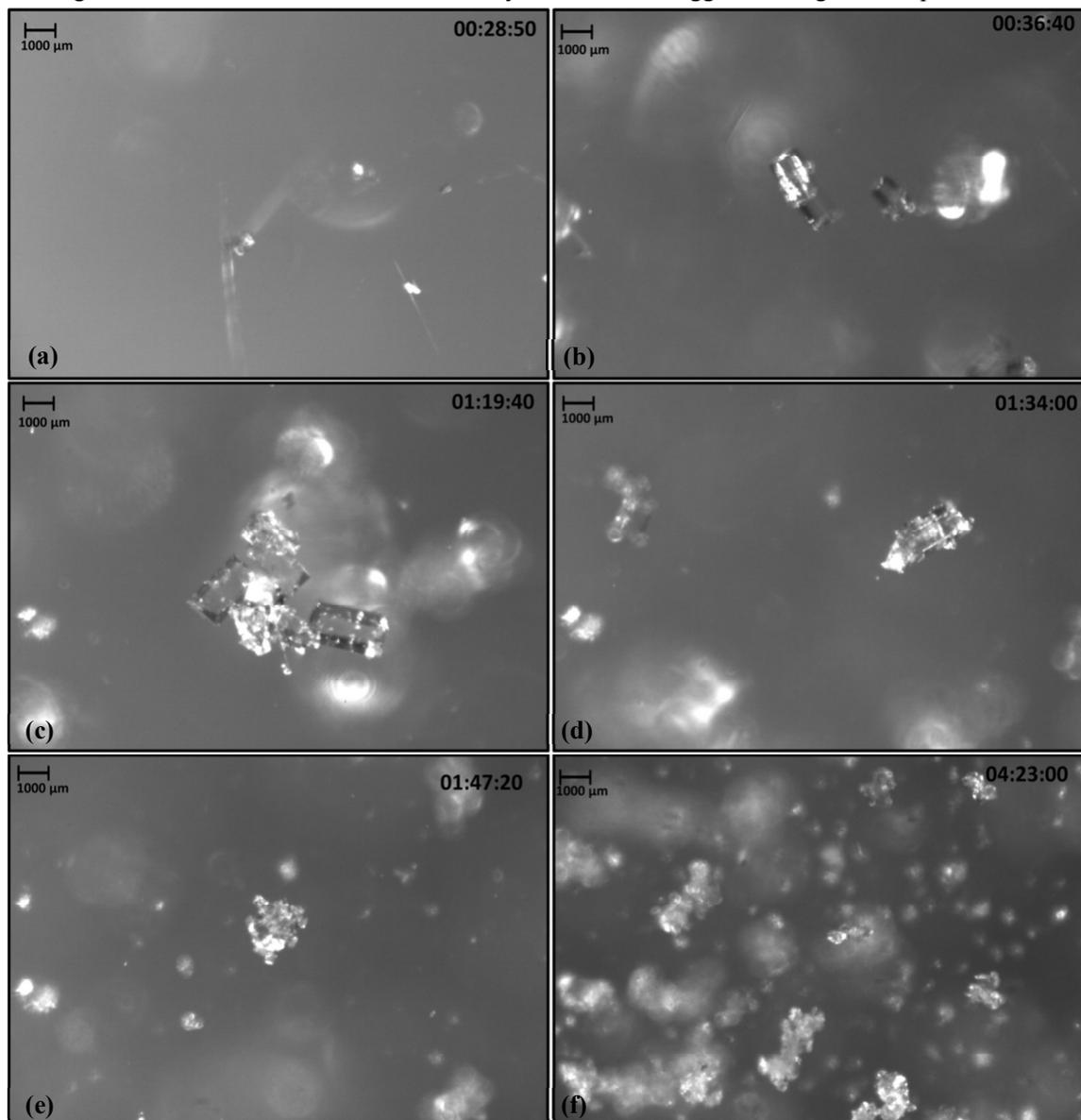


**Figure 1: PVM images from anti-solvent experiment showing crystals of (a) form II (b), (c) Form II + Form I (d) Form I + monohydrate (e), (f) Monohydrate.**

The crystals were sampled during the anti-solvent crystallization process and the microscope images (Figure 2) of the dried crystals showed that Piroxicam monohydrate formed on the surfaces of form I crystals.
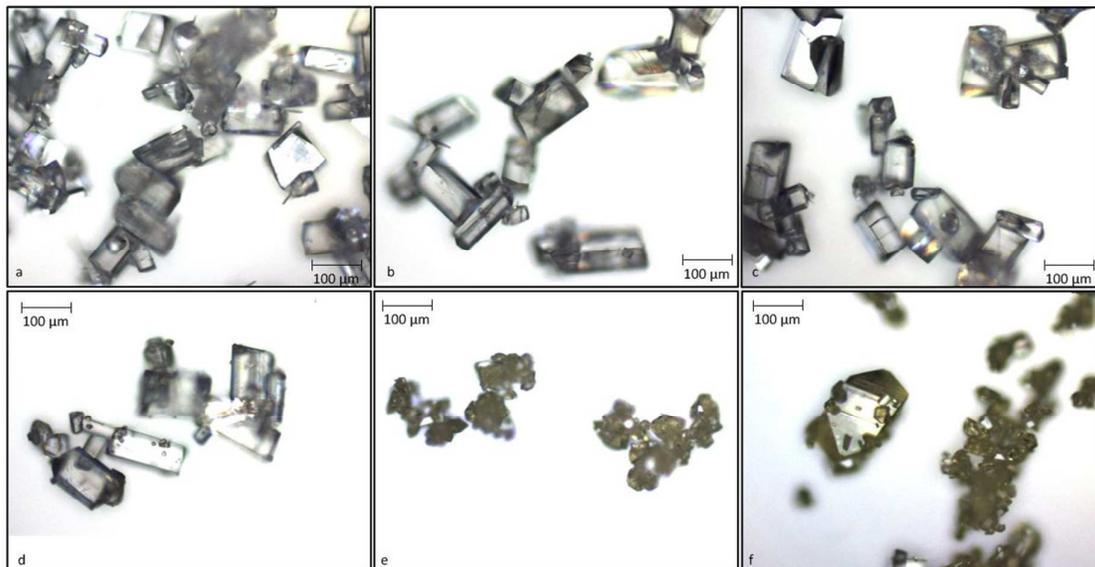


**Figure 2: Microscope images of crystal samples during anti-solvent experiment a (30 wt% water) – b/c (49 wt%) – d (61 wt%) e/f (61 wt% after 20 min. in suspension)**

The use of anti-solvent crystallization to produce form I proved to be problematic even when water addition was stopped prior to the monohydrate being observed. At 25 mg/g Piroxicam in acetone, only one experiment yielded form I without significant presence of the monohydrate form. In the two other attempts to produce form I, the monohydrate would be present to such an extent that the crystals were not deemed useful for subsequent seeding experiments (summarised in Table 2). The difference in the resulting product of the two experiments with anti-solvent addition and cooling being identical is most likely due to differences in the amount of anti-solvent that were added before nucleation was observable. The form I crystals produced in the successful batch of anti-solvent crystallization was used as seed crystals to investigate the feasibility of controlling the polymorphism of Piroxicam in cooling crystallization in the 2 L crystallizer system.

**Table 2 Experimental parameters and polymorphic form from anti-solvent experiments**

| Piroxicam concentration [mg/g] | Anti-solvent addition [ml/min] | Cooling rate [K/min] | Nucleated form |
|---|---|---|---|
| 25 | 5 | No cooling | Form I and mono-hydrate |
| 25 | 5 | 0.5 | Form I |
| 25 | 5 | 0.5 | Form I and mono-hydrate |

### 3.3 Seeding effect

It has been observed that seeding was effective for controlling polymorphism in the small scale 100 mL crystallizer[19]. For this reason seeded cooling crystallizations were conducted also to crystallize Piroxicam form I in the 2 L crystallizer. Piroxicam-acetone solutions saturated at 42°C (concentration of 45 mg/g) were prepared in order to have high yield of the process without risking boiling off of solvent. Both fixed rate cooling at -0.5°C/min and non-fixed (where the set point of the thermostat was immediately changed to 5°C once seed had been added) experiments were carried out to investigate the impact of cooling rates on the final product. The polymorphic form of the products was confirmed to be that of form I using Raman spectroscopy in all cases, and with only variations in particle size (Figure 3) was noted for the different cooling profiles. Fast cooling yielded crystals with narrow size distribution, while the linear cooling rate at -0.5°C/min gave rise to particles with larger sizes but wider size distribution. The crystals produced with fast cooling were used as seed crystals for later experiments. This ensured a uniform and narrow size distribution with fast production runs, and with particle sizes small enough to still allow for crystal growth in a stirred batch reactor in the DNC experiments.
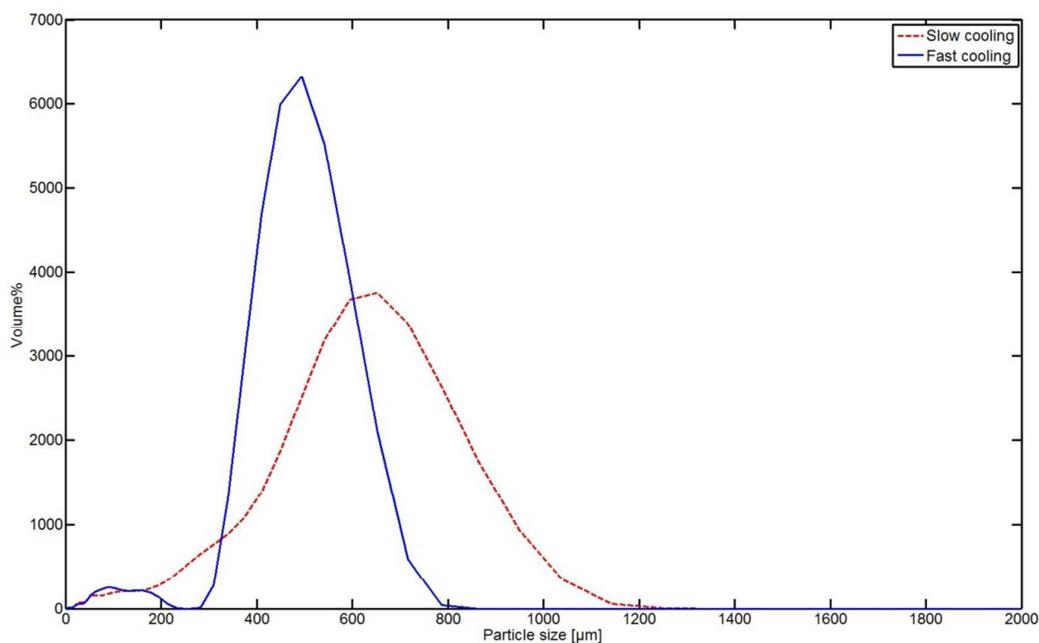


**Figure 3: Particle size distribution of crystals produced in seeded cooling crystallization with different cooling rate (Laser diffraction)**

### 3.4 DNC for improving particle size and size distribution

For the DNC experiments, Piroxicam crystals were first completely dissolved in acetone by heating the solution to 50°C. This accounts for the large spike in FBRM counts/s in Figure 4 in the first hour of the experiment until the crystals fully dissolve. Once crystals dissolved, the reactor temperature was lowered to 42°C and seed crystals (form I produced in seeded cooling crystallization with fast cooling) were added. After the crystals were dispersed in the liquid, the DNC parameters were set and control initialized. As it can be seen from Figure 4, the temperature followed the pre-set cooling profile but meanwhile would react to the counts/s from FBRM, which is considered to reflect the number of fine particles in the crystallizer. Comparing Figure 4 and Figure 5 it seems that the lower set point

for the FBRM count behaves more stable and at the end point, the FBRM count is lower than for the high DNC count. This is in agreement with the results for the particle size distributions where low DNC count also shows larger particles. Cooling would proceed if the counts/s from FBRM remained within a certain range, otherwise the temperature would increase if the counts/s from FBRM increased above the pre-defined limit, and cooling would continue until the counts/s dropped to the defined range. The control strategy is expected to minimize secondary nucleation, especially at later stage of the batch crystallization, and therefore it should lead to larger crystals with the desired polymorphism.
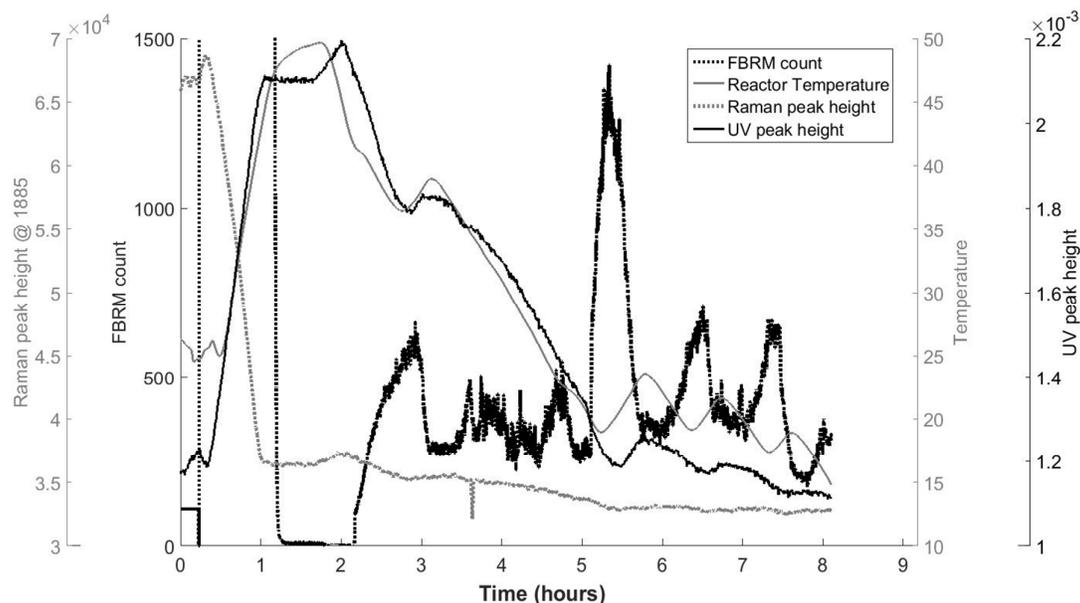


**Figure 4: Temperature profile and control signals for high set count DNC. Raman peak height is selected for peak specific for form II (Initial high FBRM count is from the mixing of Piroxicam and the solvent to prepare the saturated solution at 40°C)**
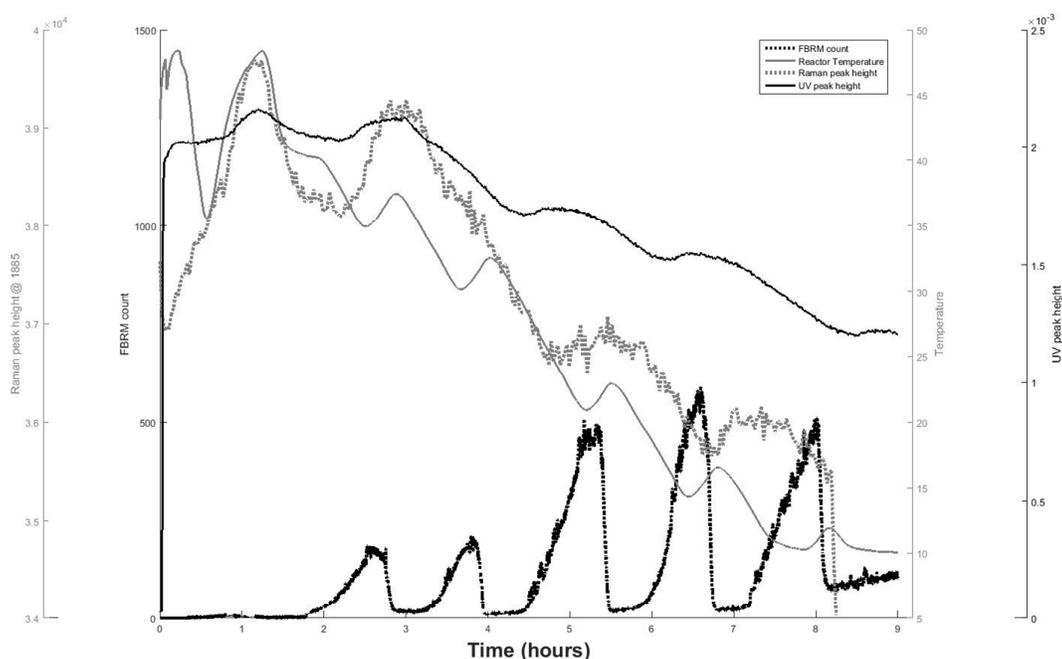


**Figure 5 Temperature profile and control signals for low set count DNC. Raman peak height is selected for peak specific for form II**

The in-line images taken with PVM have suggested that form II could occasionally crystallize out during the process. However, the needle shape of these crystals, combined with a much smaller crystal size and lower density, led to an unforeseen control option. As the DNC would respond to higher particle counts by increasing temperature till the count was within set parameters again, the DNC ended up not only improving the particle size of the crystals greatly, but also helped controlling polymorphism. As all form II crystals would contribute to the FBRM count, and only the smaller form I particles would, the system was in effect more sensitive to the formation of the form II crystals. The temperature of the reactor would thus be increased and particles would start to dissolve when form II started to nucleate. Therefore, even though form II crystals might compete with form I during the experiment, the DNC would constantly increase temperature when form II crystals nucleated and force them to dissolve again. The end result was form I crystals with a drastic increase in particle size, observable even to the naked eye. From the results from the laser diffraction particle size analyser for the seed crystals and products from the DNC experiments (Figure 6), it is seen that the control approach did have an impact on the crystal size distribution, although in the case of a high DNC count of 1000 counts/s the effect was far less pronounced as for the low count 180 count/s experiments. In both cases the polymorphic control was observed as even a count higher than what was detected from the seed crystals, where still far lower than the contribution of form 2 crystals in suspension.
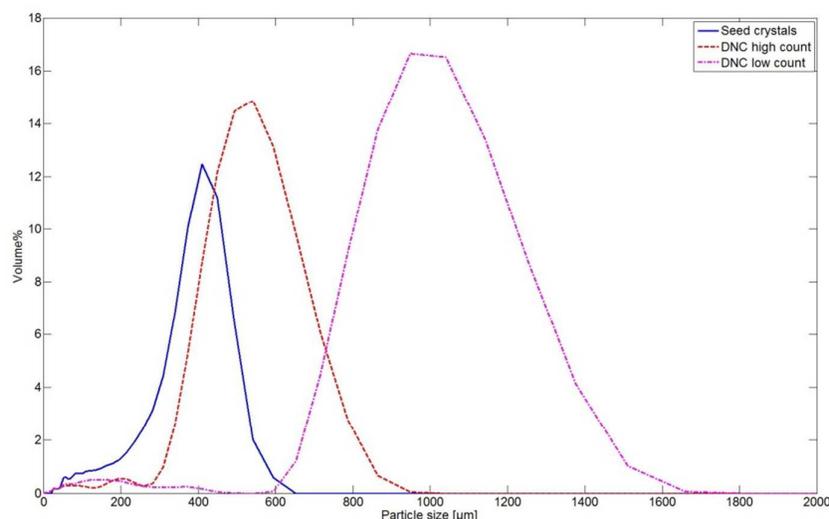


**Figure 6 Size distribution of seed and DNC crystal products (Laser diffraction).**

### 3.5 SSC

Three different SSC experiments were performed in order to determine the best conditions to allow growth of Piroxicam form I. Table 3 shows the supersaturation set-points used for the experiments and the supersaturation (SS) at the moment of seeding; initial solute concentration and seed load was the same for all experiments. The in-line monitored concentration and supersaturation profile as well as the counts/s from FBRM for the three SSC experiments are shown in Figure 7-9.

Figure 7 shows the results for Experiment 1 performed using a SS set-point of 0.00031 a.u. As shown in Figure 7a and b the SS was kept at the desired set-point for about 40 min after seeding; after that all SS was consumed by crystal growth and nucleation as shown in Figure 7c.

**Table 3: Supersaturation set-points used for the three SSC experiments.**

| Experiment | Supersaturation set point (in UV signal a.u.) | SS at seeding (in UV signal a.u.) | Final temperature (°C) |
|---|---|---|---|
| 1 | 0.00031 | 0.00039 | 10 |
| 2 | 0.0002 | 0.00041 | 5 |
| 3 | 0.00022 | 0.0002 | 10 |

The total counts/s increased rapidly between the 80 and 100 min of the experiments as the supersaturation (from 5000 to over 20000 #/sec) was consumed by secondary nucleation of form I (as confirmed by Raman microscopy at the end of the run). The decrease in total counts/s after 100 min (see Figure 7c) is due to both agglomeration of the nucleated crystals and partial sedimentation of the larger particles.

Figure 10 a and b show the CLD distribution of the crystals at the end of Experiment 1, in comparison with the seeds, and a microscopic image of the crystals. The final CLD shows the presence of fine particles indicating secondary nucleation during the experiment, while the microscopic image shows presence of agglomeration (Figure 10b). It is clear that this SS set point promotes secondary nucleation over growth; therefore, in Experiment 2 and 3 lower supersaturation set points were tested.
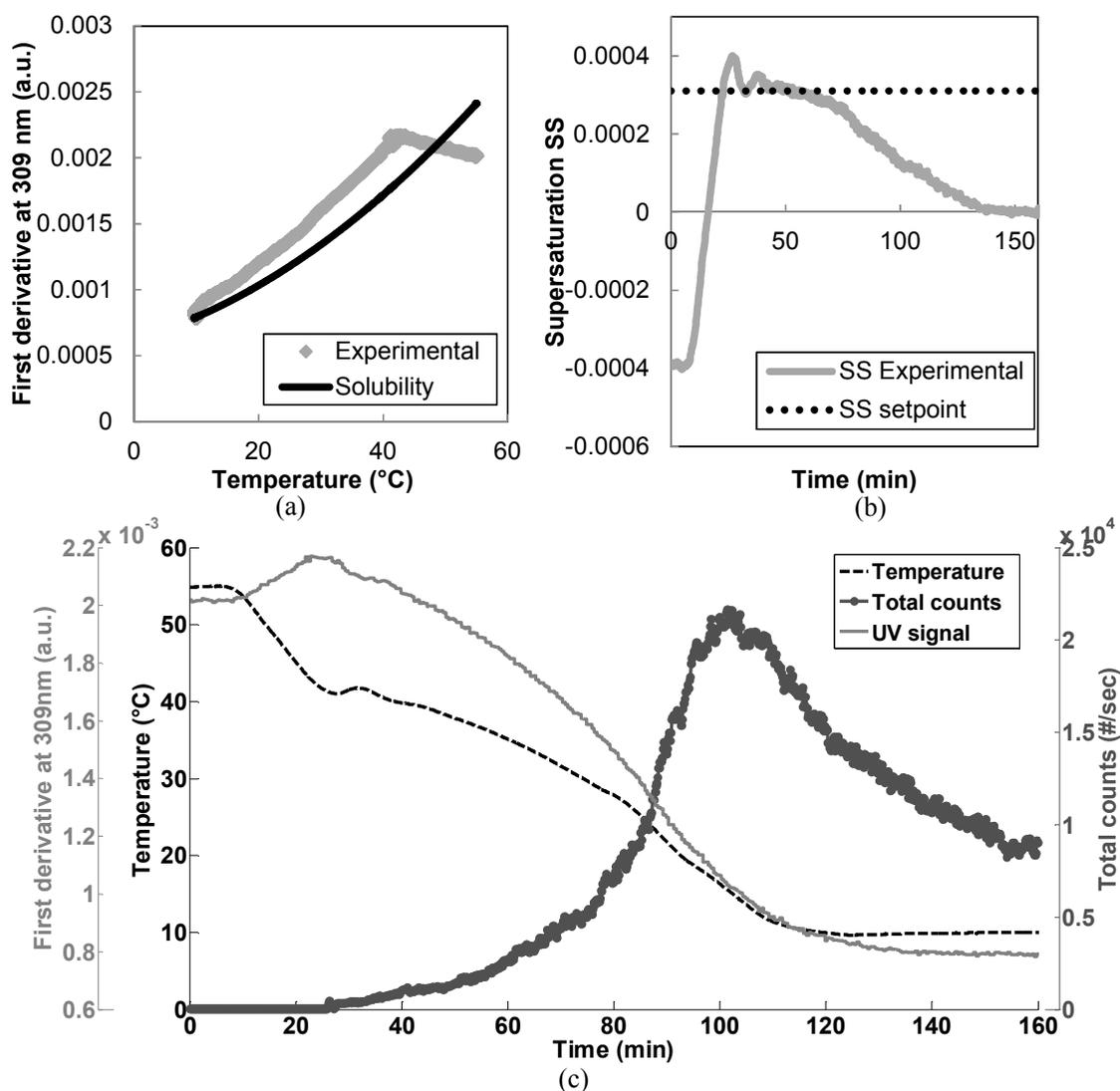
**Figure 7: Results for the SSC Experiment 1: (a) Experimental UV signal in the inferential phase diagram and solubility data (b) Supersaturation trend, measured and set point (first overshoot is created at seeding as explained in Table 3) (c) Total counts/s, temperature and UV first derivative signal as a function of time.**

Experiment 2 was conducted with similar seeding conditions compared to Experiment 1(SS at seeding was 0.00041) but using a lower SS set point. The system took around 20 min for the supersaturation to reach the SS set point, after which the level of supersaturation was kept close to the set point for about 50 min before finally decreasing to 0 as shown in Figure 8b. Secondary nucleation is still present but the maximum total counts/s is lower compared to Experiment 1 (16000 #/sec instead of over 20000 #/sec), similarly to the total amount of fines, as shown in the final CLD reported in
Figure 10a. A decrease in the total counts/s due to crystal agglomeration (similarly to Experiment 1) can be observed at the end of the run, as shown in Figure 8c. However this decrease is lower for Experiment 2 compared to Experiment 1, probably because of the lower number of fines nucleated during the run (less fines are agglomerating determining a higher final value of the total counts/s).
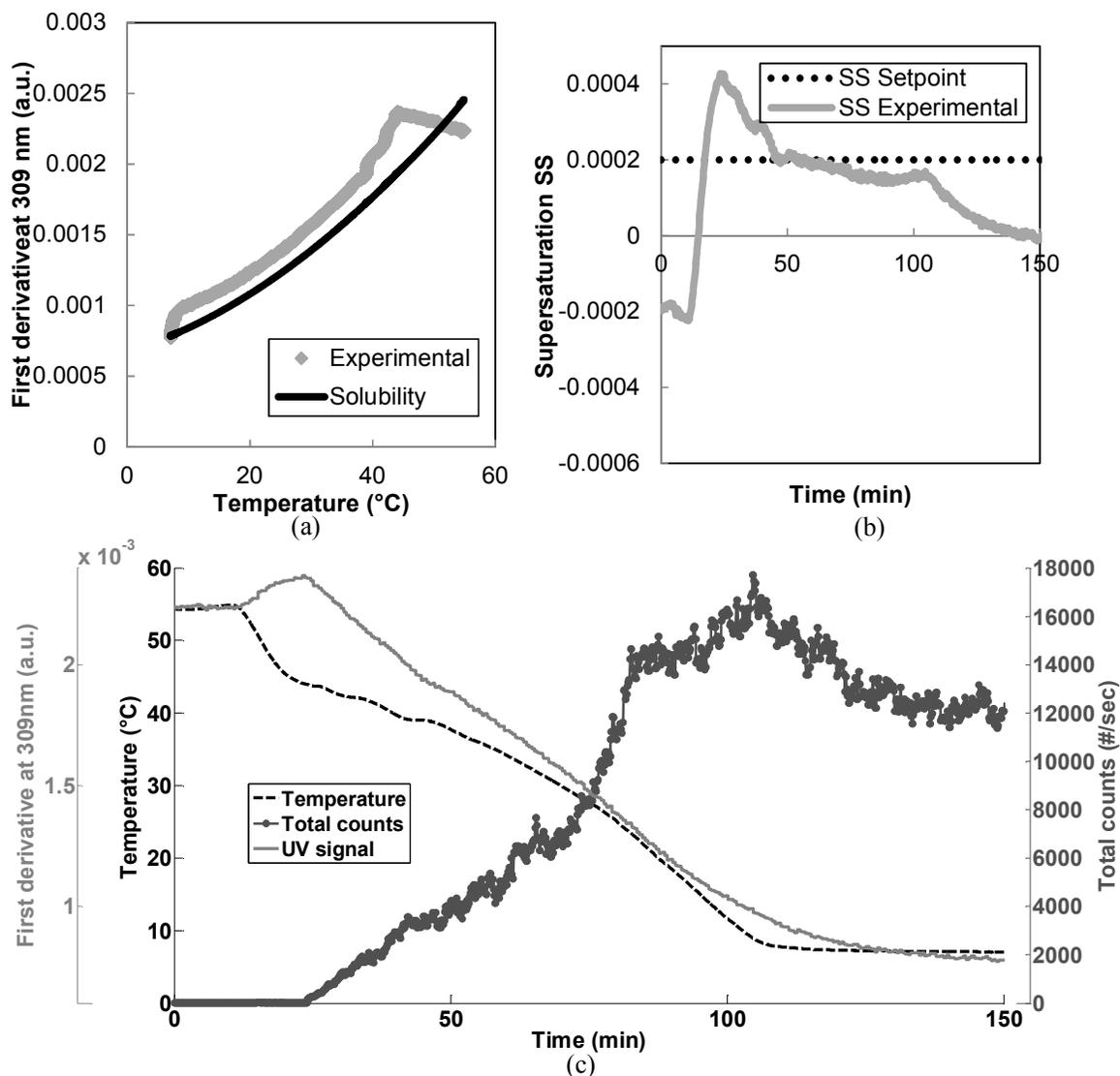
Figure 8: Results for the SSC Experiment 2: (a) Experimental UV signal in the inferential phase diagram and solubility data (b) Supersaturation trend, measured and set point (first overshoot is created at seeding as explained in Table 3) (c) Total counts/s, temperature and UV first derivative signal as a function of time.

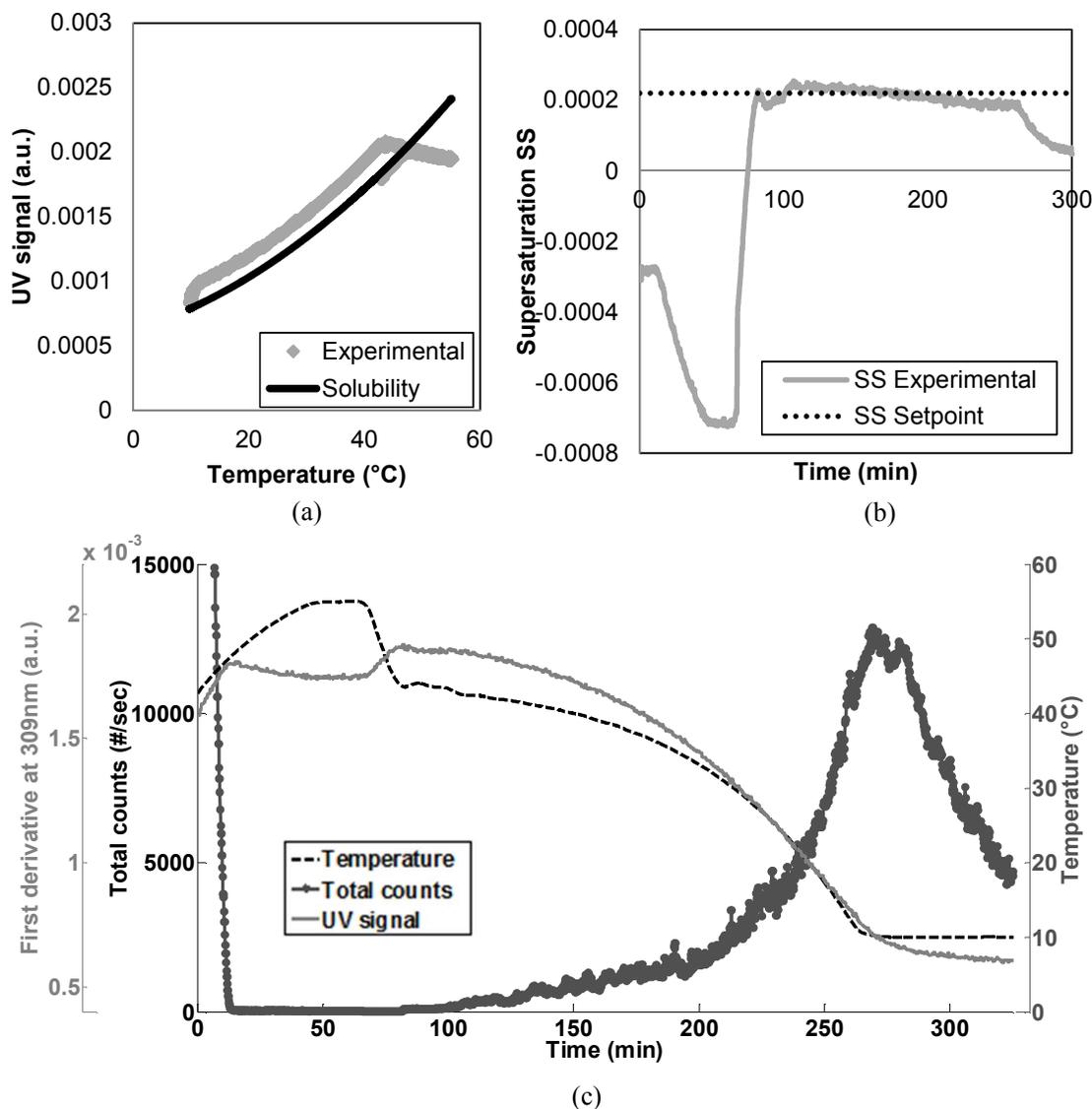(a)                                                              (b)



(c)

**Figure 9: Results for the SSC Experiment 3: (a) Experimental UV signal in the inferential phase diagram and solubility data (b) Supersaturation trend, measured and set point (first overshoot is created at seeding as explained in Table 3) (c) Total counts/s, temperature and UV first derivative signal as a function of time.**

Figure 9 shows the results obtained for Experiment 3. In this case, a supersaturation set point of 0.00022 was used and seeding was carried out at a SS level slightly lower than the SS set point (0.0002 a.u.). As shown in Figure 9 b and c this is the longest run and the SS set point was kept constant for about 175 min after seeding. However, an increase in total counts/s due to secondary nucleation is still present although less significant than that in Experiment 1 and 2 (the final value is around 12500 #/sec). Also, agglomeration of the fines happened, as proved by the decrease in total counts/s at the end of the profile and the microscopic image of Figure 10 d.
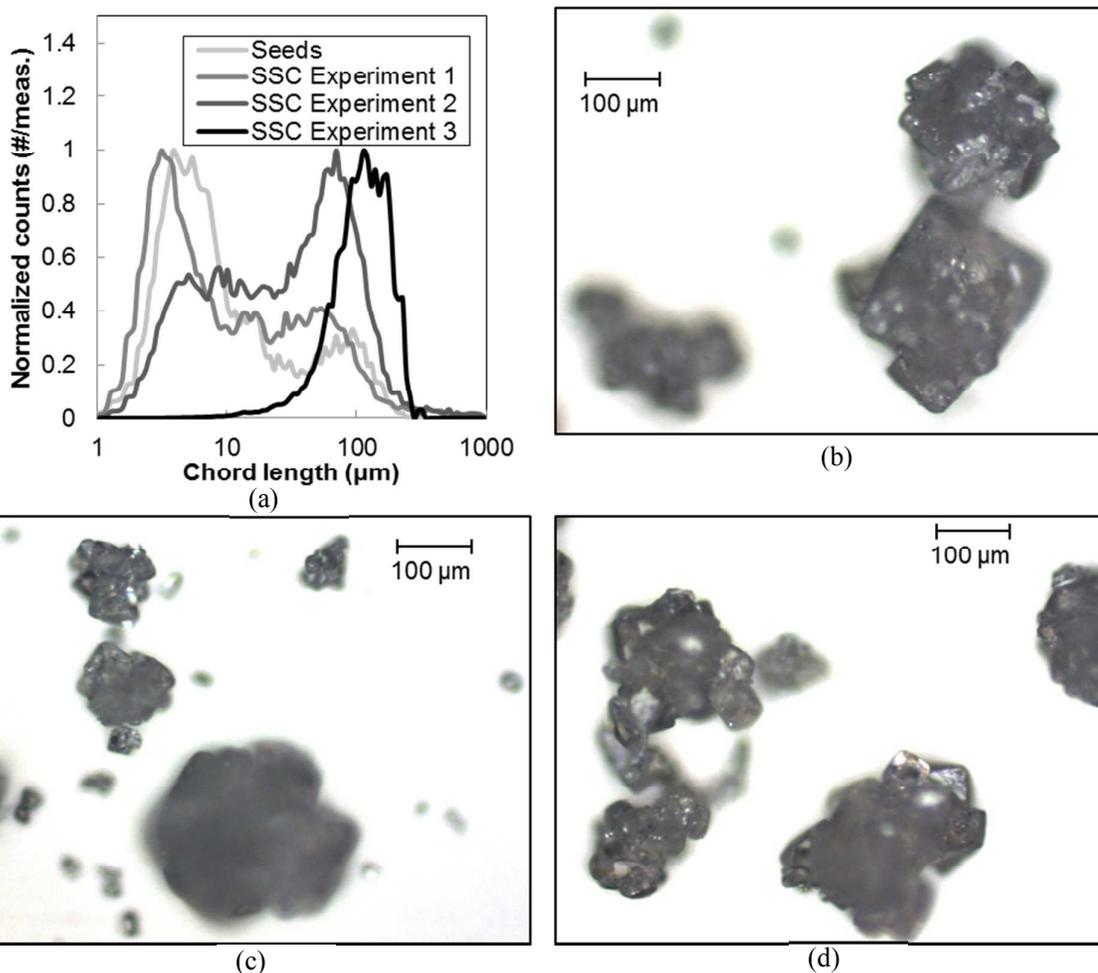
Figure 10: (a) CLDs of the seeds and at the end of Experiments 1,2 and 3 (b) Final crystals at the end of Experiment 1 (b) Final Crystals at the end of Experiment 2 (d) Final crystals at the end of Experiment 3.

It is worth noticing how, despite the clear presence of secondary nucleation, only Form I was detected by Raman spectroscopy at the end of all experiments, in contrast with the DNC experiments that showed nucleation of Form II crystals during the runs. This is probably due to the lower supersaturation imposed by the SSC during these experiments, in contrast with the DNC ones. Such lower supersaturation prevented nucleation of form II crystals favouring secondary nucleation of Form I instead.

In conclusion, SSC allowed growth of Form I crystals in a shorter time compared to DNC and without polymorphic transformation. However, this strategy couldn't minimize secondary nucleation, and agglomeration of the fines resulting in a broader CLD and lower mean size compared to the crystals produced with DNC.

## 4.   Conclusion

The complex nature of polymorphic control during crystallization process development and scaling up has been demonstrated in the present work. Although the previous investigation in the 100 ml crystallization system has suggested a strong link between the solute concentration and the nucleation of the polymorphs of Piroxicam, this result could not be reproduced in the 2L crystallizer. The simple cooling experiments did not yield the expected form, and even the anti-solvent crystallization, previously found to be a very robust method for producing form I crystals, only worked for a single run. The seeding experiments proved to be the most reliable way to produce form I in large quantities; this is in

agreement with the results obtained in the small scale experiments. The use of DNC proved to be a very effective method for significantly increasing the size of the crystals. Furthermore, the additional effect of polymorphic control when DNC was employed proved to be a great benefit. In fact, the appearance of form II crystals indicated that without DNC, this form might start competing with form I when trying to increase particle size simply with very slow cooling.

Seeded SSC experiments were also performed in order to grow pure form I. The final polymorphic purity was confirmed by Raman microscopy showing how this strategy allowed obtaining pure form I at the end of the run. However, SSC was less effective on producing larger crystals, less number of fine particles as well as less agglomerates were formed when DNC was applied to control the crystallization process.

## 5.   Acknowledgements

**6.** References

1. Lipinski, C. A., Lombardo, F., Dominy, B. W. & Feeney, P. J. Experimental and computational approaches to estimate solubility and permeability in drug discovery and development settings. *Adv. Drug Deliv. Rev.* **46,** 3–26 (2001).

2. Blagden, N., de Matas, M., Gavan, P. T. & York, P. Crystal engineering of active pharmaceutical ingredients to improve solubility and dissolution rates. *Adv. Drug Deliv. Rev.* **59,** 617–630 (2007).

3. Singhal, D. & Curatolo, W. Drug polymorphism and dosage form design: a practical perspective. *Adv. Drug Deliv. Rev.* **56,** 335–347 (2004).

4. Saifee, M., Inamda, N., Dhamecha, D. & Rathi, A. Drug polymorphism: a review. *Int. J. Health Res.* **2,** (2009).

5. Rodríguez-Hornedo, N. & Murphy, D. Significance of controlling crystallization mechanisms and kinetics in pharmaceutical systems. *J. Pharm. Sci.* **88,** 651–660 (1999).

6. Nagy, Z. K. & Braatz, R. D. Advances and New Directions in Crystallization Control. *Annu. Rev. Chem. Biomol. Eng.* **3,** 55–75 (2012).

7. Nagy, Z. K., Fevotte, G., Kramer, H. & Simon, L. L. Recent advances in the monitoring, modelling and control of crystallization systems. *Chem. Eng. Res. Des.* **91,** 1903–1922 (2013).

8. Saleemi, A. N., Rielly, C. D. & Nagy, Z. K. Comparative Investigation of Supersaturation and Automated Direct Nucleation Control of Crystal Size Distributions using ATR-UV/vis Spectroscopy and FBRM. *Cryst. Growth Des.* **12,** 1792–1807 (2012).

9. Nagy, Z. K. & Aamir, E. Systematic design of supersaturation controlled crystallization processes for shaping the crystal size distribution using an analytical estimator. *Chem. Eng. Sci.* **84,** 656–670 (2012).

10. Bakar, M. R. A., Nagy, Z. K. & Rielly, C. D. Seeded Batch Cooling Crystallization with Temperature Cycling for the Control of Size Uniformity and Polymorphic Purity of Sulfathiazole Crystals. *Org. Process Res. Dev.* **13,** 1343–1356 (2009).

11. Saleemi, A. N., Steele, G., Pedge, N. I., Freeman, A. & Nagy, Z. K. Enhancing crystalline properties of a cardiovascular active pharmaceutical ingredient using a process analytical technology based crystallization feedback control strategy. *Int. J. Pharm.* **430,** 56–64 (2012).

12. Nagy, Z. K., Aamir, E. & Rielly, C. D. Internal Fines Removal Using Population Balance Model Based Control of Crystal Size Distribution under Dissolution, Growth and Nucleation Mechanisms. *Cryst. Growth Des.* **11,** 2205–2219 (2011).

13. Saleemi, A., Rielly, C. & Nagy, Z. K. Automated direct nucleation control for in situ dynamic fines removal in batch cooling crystallization. *CrystEngComm* **14,** 2196–2203 (2012).

14. Liotta, V. & Sabesan, V. Monitoring and Feedback Control of Supersaturation Using ATR-FTIR to Produce an Active Pharmaceutical Ingredient of a Desired Crystal Size. *Org. Process Res. Dev.* **8,** 488–494 (2004).

15. Yu, Z. Q., Chow, P. S. & Tan, R. B. H. Seeding and Constant-Supersaturation Control by ATR-FTIR in Anti-Solvent Crystallization. *Org. Process Res. Dev.* **10,** 717–722 (2006).

16. Yang, Y., Song, L. & Nagy, Z. K. Automated Direct Nucleation Control in Continuous Mixed Suspension Mixed Product Removal Cooling Crystallization. *Cryst. Growth Des.* **15,** 5839–5848 (2015).

17. Yang, Y. & Nagy, Z. K. Combined Cooling and Antisolvent Crystallization in Continuous Mixed Suspension, Mixed Product Removal Cascade Crystallizers: Steady-State and Startup Optimization. *Ind. Eng. Chem. Res.* **54,** 5673–5682 (2015).

18. Yang, Y. & Nagy, Z. K. Model-Based Systematic Design and Analysis Approach for Unseeded Combined Cooling and Antisolvent Crystallization (CCAC) Systems. *Cryst. Growth Des.* **14,** 687–698 (2014).

19. Hansen, T. B. & Qu, H. Formation of Piroxicam Polymorphism in Solution Crystallization: Effect and Interplay of Operation Parameters. *Cryst. Growth Des.* **15,** 4694–4700 (2015).

20. Liu, G. *et al.* Crystallization of Piroxicam Solid Forms and the Effects of Additives. *Chem. Eng. Technol.* **37,** 1297–1304 (2014).

21. Kojić-Prodić, B. & Ruž'ć-Toroš, ž;. Structure of the anti-inflammatory drug 4-hydroxy-2-methyl-N-2-pyridyl-2H-1λ6,2-benzothiazine-3-carboxamide 1,1-dioxide (piroxicam). *Acta Crystallogr. B* **38,** 2948–2951 (1982).

22. Reck, G. *et al.* X-ray studies on piroxicam modifications. *Pharm.* **43,** 477–481 (1988).

23. Bordner, J., Richards, J. A., Weeks, P. & Whipple, E. B. Piroxicam monohydrate: a zwitterionic form, C15H13N3O4S.H2O. *Acta Crystallogr. C* **40,** 989–990 (1984).

24. Liu, G. *et al.* Stability and crystallization of piroxicam polymorphs and monohydrate phase: effects of additives. *Chem. Eng. Technol.* **Accepted for publication,** (2014).

25. Abu Bakar, M. R., Nagy, Z. K., Saleemi, A. N. & Rielly, C. D. The Impact of Direct Nucleation Control on Crystal Size Distribution in Pharmaceutical Crystallization Processes. *Cryst. Growth Des.* **9,** 1378–1384 (2008).

26. Saleemi, A. N., Rielly, C. D. & Nagy, Z. K. Comparative investigation of supersaturation and automated direct nucleation control of crystal size distribution using ATR-Uv/Vis spectroscopy and FBRM. *Cryst. Growth Des.* **12,** 1792–1807 (2012).

27. Yang, Y., Song, L. & Nagy, Z. K. Automated Direct Nucleation Control in Continuous Mixed Suspension Mixed Product Removal Cooling Crystallization. *Cryst. Growth Des.* **15,** 5839–5848 (2015).

28. Kacker, R. *et al.* Microwave Assisted Direct Nucleation Control for Batch Crystallization: Crystal Size Control with Reduced Batch Time. *Cryst. Growth Des.* **16,** 440–446 (2015).

29. Simone, E., Zhang, W. & Nagy, Z. K. Application of Process Analytical Technology-Based Feedback Control Strategies To Improve Purity and Size Distribution in Biopharmaceutical Crystallization. *Cryst. GROWTH Des.* **15,** 2908–2919 (2015).

30. Duffy, D., Barrett, M. & Glennon, B. Novel, Calibration-Free Strategies for Supersaturation Control in Antisolvent Crystallization Processes. *Cryst. Growth Des.* **13,** 3321–3332 (2013).

31. Fortunato de Carvalho Rocha, W., Sabin, G. P., Março, P. H. & Poppi, R. J. Quantitative analysis of piroxicam polymorphs pharmaceutical mixtures by hyperspectral imaging and chemometrics. *Chemom. Intell. Lab. Syst.* **106,** 198–204 (2011).